

High Energy Gamma Rays from Ultrahigh Energy Cosmic Ray Protons in Gamma Ray Bursts

Markus Böttcher^{1,2} & Charles D. Dermer²

ABSTRACT

It has recently been proposed that ultrahigh energy ($\gtrsim 10^{19}$ eV) cosmic rays (UHECRs) are accelerated by the blast waves associated with GRBs. We calculate the observed synchrotron spectrum from protons and energetic leptons formed in the cascades initiated by photopion production, taking into account $\gamma\gamma$ attenuation at the source. Normalizing to the emission characteristics of GRB 970508, we predict ~ 10 MeV - 100 GeV fluxes at a level which may have been observed with EGRET from bright GRBs, and could be detected with the proposed GLAST experiment or with ground-based air Čerenkov telescopes having thresholds \lesssim several hundred GeV. The temporal decay of the UHECR-induced high-energy γ -ray afterglows is significantly slower than that of the lower-energy burst and associated synchrotron self-Compton (SSC) radiation, which provides a direct way to test the hadronic origin of a high-energy GRB afterglow. Besides testing the UHECR origin hypothesis, the short wavelength emission and afterglows can be used to probe the level of the diffuse intergalactic infrared radiation field or constrain redshifts of GRB sources.

Subject headings: cosmic rays — gamma rays: bursts — radiation mechanisms: nonthermal

1. Introduction

The cosmological origin of GRBs has very likely been confirmed as a result of observations of GRBs with the Beppo-SAX mission. The good imaging of X-ray emission from GRBs has led to optical counterpart identification of GRB 970228 (van Paradijs et al. 1997) and GRB 970508 (Djorgovski et al. 1997). In the case of GRB 970508, observations of absorption lines in the spectrum of the optical counterpart place a lower limit on its redshift of $z = 0.835$ (Metzger et al. 1997).

The blast wave model for GRBs has met with considerable success in explaining the time dependence of the X-ray and optical afterglows (e.g., Mészáros, Rees, & Wijers 1997; Vietri 1997a;

¹Department of Space Physics and Astronomy, Rice University, 6100 Main Street, Houston, TX 77005-1892

²E. O. Hulburt Center for Space Research, Code 7653, Naval Research Laboratory, Washington, DC 20375-5352

Waxman 1997). The release of $\approx 10^{52}$ ergs of energy in a small volume results in the formation of a relativistically expanding pair fireball which transforms most of the explosion energy into the kinetic energy of baryons in a relativistic blast wave. Reconversion of the kinetic energy into radiation occurs due to collisions between different shells ejected from the central source or when the blast wave decelerates as it sweeps up matter from the external medium.

Shocks formed by these processes can accelerate protons to very high energies. If a significant fraction of the observed GRB power is transformed into UHECRs, then the measured energy density of these particles is in rough agreement with the power produced by GRBs, taking into account that UHECRs travel $\lesssim 100$ Mpc before losing a significant fraction of their energy due to photopion production with the cosmic microwave background radiation (Zatsepin & Kuzmin 1966; Greisen 1966). On the basis of such arguments, Waxman (1995a,b) and Vietri (1995) proposed that UHECRs are accelerated by GRBs. Associated $\sim 10^{14}$ eV neutrino production (Waxman & Bahcall 1997) and GeV photon production (Vietri 1997b) due to UHECR acceleration during the prompt γ -ray emission phase of the GRB have been recently predicted. Detection of neutrinos in temporal and spatial association with GRBs would confirm this cosmic ray origin theory, but will require larger neutrino detectors than presently exist.

In this *Letter*, we calculate both the prompt and delayed high energy γ -ray emission due to UHECRs accelerated in GRBs. We calculate the emergent synchrotron radiation from protons, from positrons produced in the decay of π^+ , and from pairs produced by $\gamma\gamma$ interactions. The observed emission characteristics of GRB 970508 are used to set parameter values for the blast wave model of GRBs (see Mészáros & Rees 1993; Mészáros, Rees & Papathanassiou 1994; Dermer & Chiang 1998).

2. Evolution of GRB Blast Wave

After reaching a maximum speed defined by the baryon content and total energy of the explosion, the Lorentz factor Γ of a relativistic blast wave evolves by sweeping up matter from its surrounding medium (Blandford & McKee 1976; Mészáros & Rees 1993). For a blast wave of total energy $E = 10^{52} E_{52}$ erg, which expands with initial bulk Lorentz factor $\Gamma_0 = 300 \Gamma_{300}$ into a medium of uniform density $n_0 \text{ cm}^{-3}$, the coasting phase ends and the deceleration phase begins when the blast wave has a characteristic radius given by

$$x_0 = 2.6 \cdot 10^{16} \left(\frac{E_{52}}{n_0 \Gamma_{300}^2} \right)^{1/3} \text{ cm} \quad (1)$$

(Rees & Mészáros 1992). For $x > x_0$, the bulk Lorentz factor follows the power-law behavior $\Gamma(x) = \Gamma_0 (x/x_0)^{-g}$ where, for a uniform density medium, $g = 3/2$ in the non-radiative regime when transformation of the internal energy of swept-up particles into radiation is inefficient, and $g = 3$ in the radiative regime where the internal energy is efficiently radiated.

According to the scenario of UHECR acceleration by GRB blast waves (Vietri 1995; Waxman 1995a,b), we assume that a fraction ξ of the energy in nonthermal protons in the blast wave region is transformed into a power-law distribution $N_{\text{cr}}(\gamma_{\text{cr}}; x) = K_{\text{cr}}(x)\gamma_{\text{cr}}^{-s}$ of ultrarelativistic cosmic ray protons with Lorentz factors $\Gamma(x) \leq \gamma_{\text{cr}} \leq \gamma_{\text{cr,max}}$ in the fluid frame comoving with a small element of the blast wave region. Here

$$K_{\text{cr}}(x) = \frac{1}{m_p c^2} \frac{\xi E_p(x) (2-s)}{\gamma_{\text{cr,max}}^{2-s} - \Gamma(x)^{2-s}}, \quad (2)$$

where $E_p(x)$ is the energy in non-thermal protons swept up from the external medium, and the maximum cosmic-ray Lorentz factor is

$$\gamma_{\text{cr,max}} \simeq 10^{10} E_{52}^{1/3} \Gamma^{-2/3} n_0^{1/6} \zeta^{1/2} r^{1/2} \quad (3)$$

(Vietri 1995, 1997b). The term ζ in this equation is the equipartition factor for the magnetic field, given through the expression

$$H(\text{G}) = (8\pi r m_p c^2 n_0)^{1/2} \Gamma \zeta^{1/2} \cong 0.6 \Gamma[(r/10) n_0 \zeta]^{1/2}, \quad (4)$$

and r is the compression ratio which can exceed 4 for relativistic shocks or in shocks where nonlinear feedback of the nonthermal particle pressure affects the shock structure (e.g., Ellison, Jones, & Reynolds 1990). We let $\xi = 1$, $r = 10$, and $\zeta = 1$ in our calculations. The choice of $\zeta \sim 1$ is needed for Fermi acceleration to be efficient enough to produce cosmic-ray protons of $E_p \sim 10^{20}$ eV (Vietri 1995).

Finally, we have to relate the measured flux at a given time to the comoving differential photon density $n_{\text{ph}}(\epsilon)$, where $\epsilon = E_\gamma/(m_e c^2)$ is the dimensionless photon energy. The observed radiation is a convolution of the contributions from regions of the blast wave emitting at different times and moving with different Lorentz factors and directions with respect to the observer (Rees 1967). The completely self-consistent transformation to the observer's frame can therefore in general only be done numerically, taking into account the evolution of the intrinsic radiation spectrum. However, due to the very strong Doppler enhancement along the direction of motion in a relativistic blast wave, only a small fraction of the blast wave covering a solid angle of order $1/\Gamma^2$ contributes significantly to the observed radiation, within which the difference in light travel time to the observer is negligible. Within this approximation, an observed power-law spectrum given by $S_{\text{obs}}(\epsilon_{\text{obs}}) = S_0 \epsilon_{\text{obs}}^{-\alpha}$ between $\epsilon_{\text{obs},1} \leq \epsilon_{\text{obs}} \leq \epsilon_{\text{obs},2}$ is related to the spectral photon density in the comoving frame, given by $n_{\text{ph}}(\epsilon) = n_{\text{ph}}^0 \epsilon^{-(1+\alpha)}$ between $\epsilon_1 = (1+z)\epsilon_{\text{obs},1}/(2\Gamma) \leq \epsilon \leq (1+z)\epsilon_{\text{obs},2}/(2\Gamma) = \epsilon_2$, through the expression

$$n_{\text{ph}}^0 \cong \frac{4 d_L^2 S_0 (1+z)^{\alpha-1}}{c x^2 m_e c^2 (2\Gamma)^{1+\alpha}}. \quad (5)$$

Here, d_L is the luminosity distance.

3. Photopion Production, Proton Synchrotron Radiation and Pair Cascades

We calculate the γ -ray and positron production spectra from decaying pions produced by UHECRs interacting with photons (see, e.g., Stecker 1979). The UHECR energy-loss rate through photopair production is much smaller than that of photopion production for the proton energies and photon spectra considered here, and will be neglected. The differential cross section for photopion production is approximated by $d\sigma/d\epsilon' \approx \sigma_0 \delta(\epsilon' - E_\Delta/m_e c^2)$, where $\sigma_0 = 2 \cdot 10^{-28} \text{ cm}^2$, $\epsilon' \cong \gamma_{\text{cr}} \epsilon (1 - \mu)$ is the photon energy in the proton rest frame, and $E_\Delta \cong 330 \text{ MeV}$. Noting that pions are produced primarily near threshold in the protons' rest frame (i. e., $\gamma_\pi \approx \gamma_{\text{cr}}$), we obtain the pion production rate

$$\begin{aligned} \dot{N}_\pi(\gamma_\pi) &= \frac{c}{2} \int_1^\infty d\gamma_{\text{cr}} N_p(\gamma_{\text{cr}}) \int_{-1}^1 d\mu \int_0^\infty d\epsilon n_{\text{ph}}(\epsilon) (1 - \beta_p \mu) \frac{d^2\sigma}{d\mu d\gamma_\pi} \\ &\approx \sigma_0 n_{\text{ph}}^0 \frac{c K_{\text{cr}} E_\Delta}{2 m_e c^2 (\alpha + 1)} \gamma_\pi^{-(1+s)} \left\{ \left[\max \left(\epsilon_1, \frac{E_\Delta}{2 \gamma_\pi m_e c^2} \right) \right]^{-(\alpha+1)} - \epsilon_2^{-(\alpha+1)} \right\} \\ &\quad \cdot \Theta \left\{ \gamma_\pi; \max \left[\Gamma(x), \frac{E_\Delta}{2 m_e c^2 \epsilon_2} \right], \gamma_{\text{cr,max}} \right\}. \end{aligned} \quad (6)$$

The generalized Heaviside function Θ is defined as $\Theta(x; a, b) = 1$ if $a \leq x \leq b$, and 0 otherwise. The photon spectrum from decaying neutral pions is then

$$\begin{aligned} \dot{N}_\gamma^{\pi^0 \rightarrow 2\gamma}(\epsilon) &= \sigma_0 n_{\text{ph}}^0 \frac{c K_{\text{cr}} E_\Delta}{2 m_\pi c^2 (\alpha + 1)} \\ &\quad \cdot \int_{\max[\epsilon m_e/m_\pi, \Gamma(x), E_\Delta/(2 \epsilon_2 m_e c^2)]}^{\gamma_{\text{cr,max}}} d\gamma_\pi \gamma_\pi^{-(2+s)} \left\{ \left[\max \left(\epsilon_1, \frac{E_\Delta}{2 \gamma_\pi m_e c^2} \right) \right]^{-(\alpha+1)} - \epsilon_2^{-(\alpha+1)} \right\}. \end{aligned} \quad (7)$$

For simplicity, we assume that charged pions are produced at the same rate (Eq. [6]) as π^0 s and, after decaying into one positron and three neutrinos, on average 1/4 of the energy of the pion is carried by the positron (instead of 1/2 carried by each of the two photons in the case of π^0 decay). This yields $\dot{N}_{e^+}(\gamma_+) \approx \dot{N}_\gamma^{\pi^0 \rightarrow 2\gamma}(2\gamma_+)$ for the first generation of relativistic positrons injected into the shock region. We take into account energy losses due to synchrotron radiation, but neglect escape, pair annihilation, and Compton losses. Escape is unlikely given the small Larmor radius, and pair annihilation is only important for low-energy positrons which radiate inefficiently. Compton losses are found to be much less important than synchrotron losses for the parameters used here. Integration of the continuity equation yields the “steady-state” distribution of the first generation of positrons.

The proton synchrotron spectrum is calculated using a δ -function approximation for the emission of a single proton, giving

$$\dot{N}_\gamma(\epsilon) = \frac{c\sigma_T H_c^2}{(27\pi m_e c^2)} \left(\frac{\epsilon_{H,p}}{\epsilon}\right)^{1/2} N_{\text{cr}} \left(\sqrt{\frac{\epsilon}{\epsilon_{H,p}}}\right), \quad (8)$$

where $\epsilon_{H,p} = (3/2)(m_e/m_p) H/H_c$, and $H_c = 4.414 \cdot 10^{13}$ G.

We compute the opacity $\tau_{\gamma\gamma}$ using the full pair production cross section and assuming that the shell width $\delta x_{\text{sh}} = x/\Gamma$ (Mészáros, Laguna, & Rees 1993). The shock region is optically thick to $\gamma\gamma$ pair production on the soft burst and afterglow radiation for photons with $E_\gamma \gtrsim 100$ GeV. This differs from the results of Waxman & Bahcall (1997) and Vietri (1997b), who find the region to be optically thick for photons above ~ 100 MeV and ~ 1 TeV, respectively. This difference is largely due to the smaller size scale used by Waxman & Bahcall and the different nominal values of the Lorentz factors ($\Gamma_{300} = 1/3, 1,$ and 3 in Waxman & Bahcall, this study, and Vietri, respectively). The $\gamma\gamma$ absorbed portion of the high-energy photons initiates a pair cascade. Since most of the secondary pairs of the electromagnetic cascade are injected at high energies, the steady-state pair distribution of secondary particles can be approximated by a power-law with index 2 over a wide range of electron/positron energies. This yields a synchrotron spectrum of spectral index $\alpha_{\text{syn}} = 1/2$. We approximate the radiative output of the cascade by a $\gamma\gamma$ -absorbed power-law spectrum of energy index $1/2$ containing the energy of the absorbed high-energy photons from π^0 decay and synchrotron radiation of the first generation of positrons from π^+ decay.

SSC radiation from the primary electrons may also play an important role. The numerical simulations described in Chiang & Dermer (1998) were used to determine the expected level and energy range of the SSC component. Note that the SSC component is significantly weaker than estimated using simple Thomson-limit arguments because Klein-Nishina effects are very important in this case.

4. Numerical results

For the purpose of illustration, we compute the expected high-energy prompt radiation and afterglow from GRB 970508. We approximate its observed spectrum during the burst phase by a broken power-law with energy index $\alpha_1 = 0$ below $E_{\text{break}} \approx 45$ keV and $\alpha_2 = 1$ above the break, fitting to the Beppo-SAX fluxes measured in the 2-26 keV and 40-700 keV bands during the first 25 s of the GRB (Piro et al. 1998). The spectrum is assumed to extend from $E_{\text{obs},1} = 1$ eV, corresponding to the self-absorption frequency early in the GRB, to $E_{\text{obs},2} = 10$ MeV (the calculations do not depend sensitively on the upper energy). We assume $E = 10^{52}$ erg, $z = 0.835$, $\Gamma_0 = 300$. Eq. (3) implies that the cosmic-ray spectrum extends up to $\gamma_{\text{cr,max}} = 7 \cdot 10^8$, and we assume that it has a spectral index of $s = 2$. Fig. 1 shows the different components of the resulting broad-band spectrum at the point x_0 , and the pair production opacity $\tau_{\gamma\gamma}$ at this point.

Examining synchrotron losses in the evolving magnetic field (eq. [4]), one finds that only particles with $\gamma \lesssim 5(m/m_e)^3 / [(r/10)\zeta n_0^{2/3} \Gamma_{300}^{1/3} E_{52}^{1/3}]$ cool efficiently through synchrotron processes.

Thus synchrotron cooling is very inefficient for protons, though electrons cool efficiently if $\zeta \approx 1$. The radiative output of protons is dominated by synchrotron radiation rather than photo-pion production, although the efficiency of the latter process can be increased in a colliding shell scenario (e.g., Waxman & Bahcall 1997).

Approximating the observed evolution of the optical to soft γ -ray spectrum of the GRB and the afterglow from GRB 970508, we assume that the flux remains constant for $t_0 = 30$ s in the observer’s frame and then decays as $S(t) = S_0 (t/t_0)^{-1.07}$. The break energy E_{break} and the upper cut-off E_2 are assumed to decrease with the same temporal behavior. Because cooling is inefficient, we expect that the evolution of the blast wave is more closely described by the non-radiative limit. Fig. 2 illustrates the time dependence of the high-energy γ -ray afterglow, compared to the evolution of the low-energy burst and the SSC radiation in this case. The high-energy afterglow decays much more slowly than the optical-to-X-ray afterglow and the SSC component. In the radiative case, the proton synchrotron afterglow radiation decays much faster than in the non-radiative case, but still considerably less rapidly than the optical-to-X-ray afterglow.

The temporal behavior of the uncooled proton synchrotron flux in the evolving field (4) goes as $t_{\text{obs}}^{-\chi}$ where $\chi_{\text{uncooled}} = [4g + (7\eta/4) - 3]/(1 + 2g)$ for $s = 2$ and an external medium $n_{\text{ext}} \propto x^{-\eta}$ (see Dermer & Chiang 1998, eqs. [50], [51]). In the cooled regime, characteristic of the electron synchrotron radiation, we find $\chi_{\text{cooled}} = (4g + \eta - 2)/(1 + 2g)$. In the non-radiative $g = 3/2$ regime with $\eta = 0$, we find that $\chi_{\text{uncooled}} = 3/4$ and $\chi_{\text{cooled}} = 1$. The effects of the cascade cause the high-energy radiation to decay even more slowly than estimated by these analytic expressions.

The level of the proton synchrotron flux is not strongly dependent on the endpoints of the low-energy spectrum because this component is produced mainly at energies where intrinsic $\gamma\gamma$ attenuation is unimportant. The photopion component is, however, reduced when the high-energy cutoff of the burst emission is decreased. Due to the smaller $\gamma\gamma$ optical depth, a smaller portion of the high-energy radiation resulting from π^0 decay and synchrotron emission of first-generation positrons is absorbed and transferred to the cascade. Different values of Γ_0 significantly change the energy range and amplitude of the emergent proton synchrotron and photopion emission, but only during the early portion of the GRB. At comparable times later in the GRB, the flux and energy ranges are similar.

5. Discussion

The high energy γ radiation from proton synchrotron and the photopion-induced pair cascade decays more slowly than the low energy afterglow and the SSC radiation, because cooling is inefficient for protons whereas electrons cool efficiently. Therefore, synchrotron radiation from protons can be distinguished from direct electron synchrotron or SSC emission by comparing the temporal decay rates in the afterglow phase, even though the SSC radiation is produced at roughly the same flux levels as the proton synchrotron radiation early in the GRB. A monotonically

increasing ratio of the high-energy γ -ray flux to the optical or soft X-ray flux in the GRB afterglow would provide strong evidence for proton synchrotron radiation and UHECR acceleration in GRBs.

The flux sensitivities of EGRET and GLAST (pointed mode) for an $\alpha = 1$ spectrum are $\approx 8 \cdot 10^{-8}$ ph (> 100 MeV) $\text{cm}^{-2} \text{s}^{-1}$ and $\approx 2 \cdot 10^{-9}$ ph (> 100 MeV) $\text{cm}^{-2} \text{s}^{-1}$, respectively (Kurfess et al. 1997; GLAST 1997). In the inset to Fig. 2, we compare the fluence sensitivities of EGRET, GLAST and Whipple to the fluence predicted by our calculations of GRB 970508. The calculated > 100 MeV burst fluence is an order of magnitude below the EGRET sensitivity level, but could be detected in brighter GRBs. GLAST, when operated in the pointed mode, would be able to detect the > 100 MeV γ -ray afterglow at the predicted level. The emission from UHECRs accelerated in GRBs may already have been observed in six bright BATSE bursts that were detected with EGRET (Dingus 1995; Catelli, Dingus, & Schneid 1996; Hurley et al. 1994) and display weak evidence for a hard tail at > 100 MeV and GeV energies. From Fig. 2, we note that the best opportunity for detection of ~ 100 MeV emission with EGRET or GLAST is within the first several minutes of the GRB whereas a larger fraction of the high-energy gamma-ray emission is produced on time scales of hours, which is in accord with the detection of an 18 GeV photon from GRB 940217 90 minutes after the main part of the GRB (Hurley et al. 1994).

Fig. 2 indicates weak delayed > 100 GeV-TeV emission, which is below the thresholds of existing Čerenkov telescopes. This emission would not, in any case, be detectable from a GRB located at a redshift $z \gtrsim 0.5$ (see Stecker & de Jager 1997; Salamon & Stecker 1998) due to absorption by the intergalactic infrared radiation field, but could be detected from nearby bright GRBs. The delayed afterglows in the 10-100 GeV range from such GRBs could provide a way to measure the level of the infrared background radiation and to yield upper limits on redshifts, but will require high sensitivity ground-based Čerenkov telescopes with low energy thresholds. If redshifts are independently measured, cutoffs in the observed high energy radiation spectrum can be used to infer the level of the infrared background.

The photopion process could be more important during the early phase of the GRB if the size scale of the system is determined by collisions between shells (Waxman & Bahcall 1997). In this case, we would expect a considerably larger > 10 MeV flux due to the photopion/ $\gamma\gamma$ cascade during the primary γ -ray emission phase. Flux levels of high-energy γ radiation could therefore constrain the expected level of neutrino production from UHECRs and discriminate between the colliding shell and external shock scenario of GRBs (Vietri 1997b).

We thank J. Chiang for useful discussions and the anonymous referee for a detailed and constructive report. MB acknowledges support by the German Academic Exchange Service (DAAD). The work of CD is supported by the Office of Naval Research and the *Compton Gamma Ray Observatory* Guest Investigator program.

REFERENCES

- Blandford, R. D., & McKee, C. F. 1976, *Phys. Fluids*, 19, 1130
- Catelli, J. R., Dingus, B. L., & Schneid, E. J. 1996, in the Third Huntsville Symposium on Gamma Ray Bursts, ed. C. Kouveliotou, M. F. Briggs, & G. J. Fishman (New York: AIP), 158
- Chiang, J., & Dermer, C. D. 1998, *ApJ*, submitted (astro-ph/9803339)
- Dermer, C. D., & Chiang, J. 1998, *New Astronomy*, 3, 157
- Dingus, B. L. 1995, *A&SS*, 231, 187
- Djorgovski, S. G., et al. 1997, *Nature*, 387, 876
- Ellison, D. C., Jones, F. C., & Reynolds, S. P. 1990, *ApJ*, 360, 702
- GLAST 1997, <http://www-glast.stanford.edu>
- Greisen, K. 1966, *PRL*, 16, 748
- Hurley, K. C., et al. 1994, *Nature*, 372, 652
- Kurfess, J. D., Bertsch, D. L., Fishman, G. J., & Schönfelder, V. 1997, in The Fourth Compton Symposium, ed. C. D. Dermer, M. S. Strickman, & J. D. Kurfess (New York: AIP), 509
- Mészáros, P., & Rees, M. J. 1993, *ApJ*, 405, 278
- Mészáros, P., Laguna, P., & Rees, M. J. 1993, *ApJ*, 415, 181
- Mészáros, P., Rees M. J., & Papathanassiou, H. 1994, *ApJ*, 432, 181
- Mészáros, P., Rees, M. J., & Wijers, R. A. M. J., 1997, *ApJ*, submitted (astro-ph/9709273)
- Metzger, M. R., et al. 1997, *Nature*, 387, 878
- Piro, L., et al. 1998, *A&A*, 331, L41
- Rees, M. J., & Mészáros, P., 1992, *MNRAS*, 258, 41P
- Rees, M. J. 1967, *Nature*, 211, 468
- Salamon, M. H., & Stecker, F. W. 1998, *ApJ*, 493, 547
- Stecker, F. W., 1979, *ApJ*, 228, 919
- Stecker, F. W., & de Jager, O. C. 1997, *ApJ*, 476, 712
- van Paradijs, J., et al. 1997, *Nature*, 386, 686
- Vietri, M. 1997a, *ApJ*, 478, L9
- Vietri, M. 1997b, *PRL* 78, 23, 4328
- Vietri, M. 1995, *ApJ*, 453, 883
- Waxman, E. 1997, *ApJ*, 485, L5
- Waxman, E. 1995a, *PRL*, 75, 386
- Waxman, E. 1995b, *ApJ*, 452, L1

Waxman, E., & Bahcall, J. 1997, PRL, 78, 2292

Zatsepin, G. T., & Kuzmin, V. A. 1966, JETP Lett., 4, 78

This preprint was prepared with the AAS L^AT_EX macros v4.0.

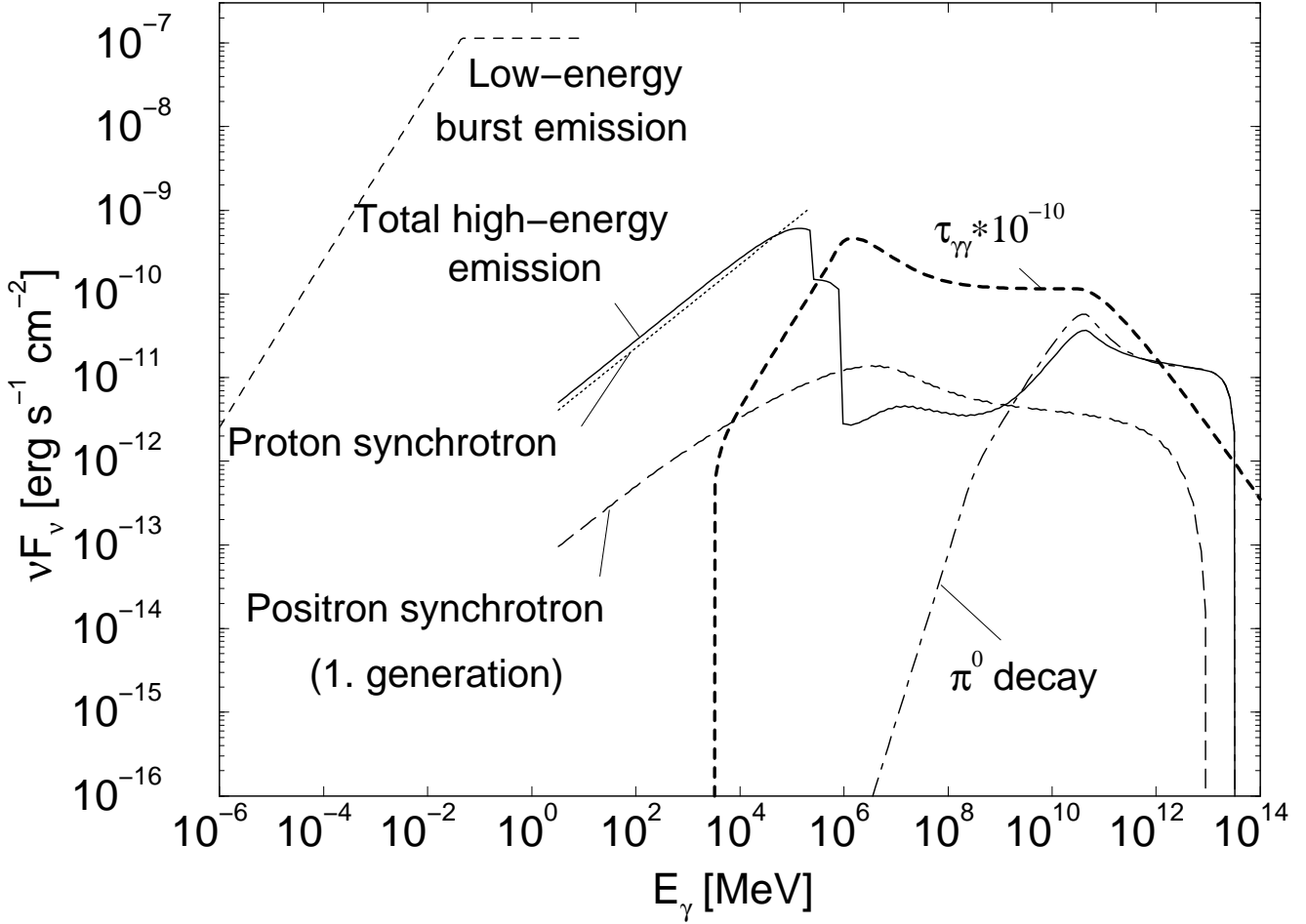


Fig. 1.— Broadband spectrum of a GRB blast wave at the point x_0 of transition to the asymptotic regime, for parameters derived from the observations of GRB 970508. Dashed: optical to soft γ -ray spectrum; dotted: proton synchrotron radiation; long dashed: synchrotron radiation from positrons produced in π^+ decay; dot-dashed: π^0 decay; solid: total high-energy spectrum, including $\gamma\gamma$ absorption and synchrotron emission from the pair cascade; thick dashed: $\gamma\gamma$ pair production opacity multiplied by 10^{-10} .

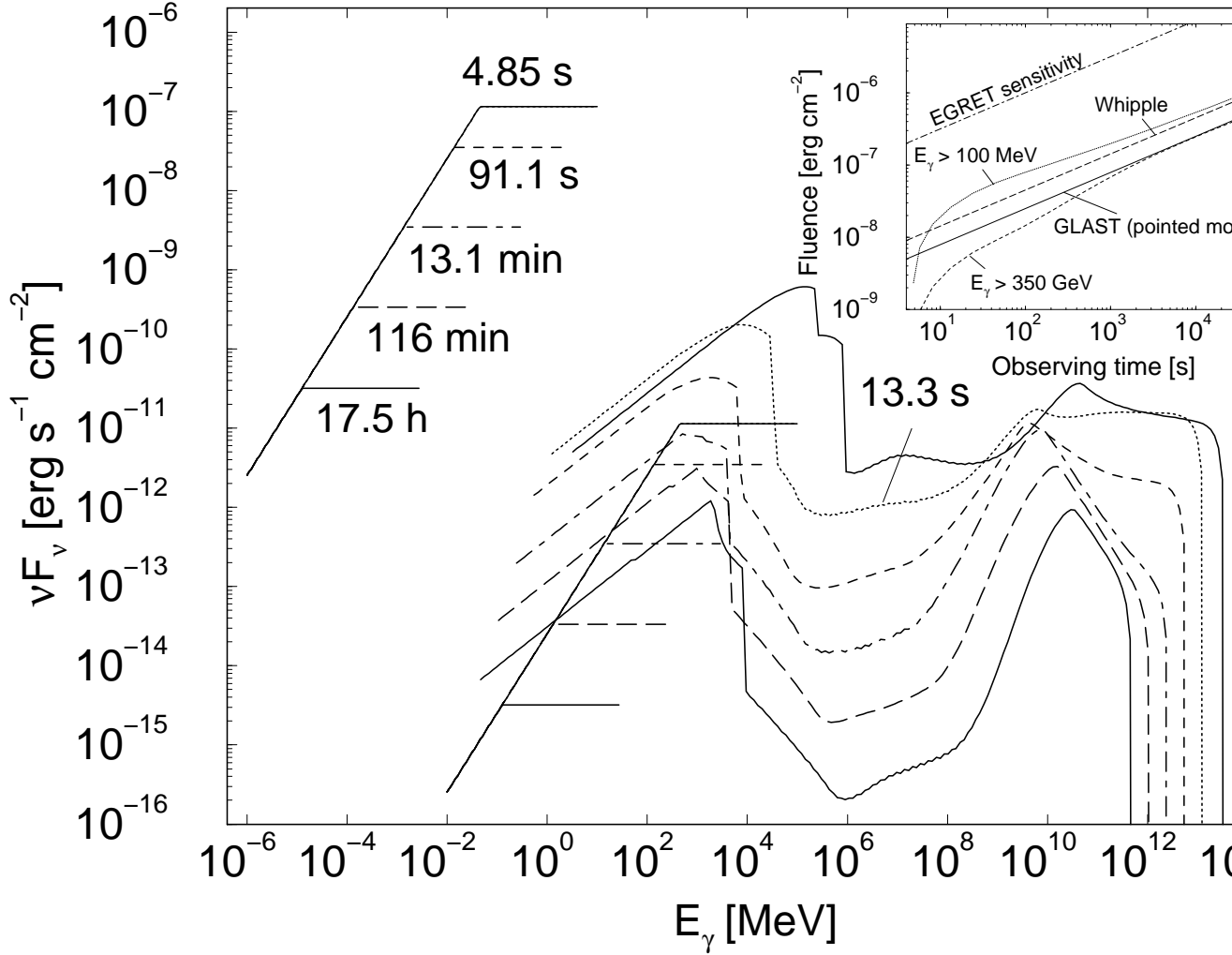


Fig. 2.— Time history of the broadband burst and afterglow emission in the non-radiative regime at different observer times. The expected SSC radiation associated with the low-energy burst emission is shown for comparison. The inset shows time- and energy-integrated fluxes for high energy emission from GRB 970508 for energies > 100 MeV (dotted curve) and > 350 GeV (short-dashed curve). The dot-dashed, solid and long-dashed line are the fluence sensitivities for EGRET, GLAST in its pointed mode, and Whipple, respectively.